

INVESTIGATION OF THE WEATHERING EFFECT ON THE ^{40}Ar - ^{39}Ar AGES OF ANTARCTIC METEORITES

Ichiro KANEOKA

*Geophysical Institute, Faculty of Science, University of Tokyo,
Yayoi 2-chome, Bunkyo-ku, Tokyo 113*

Abstract: In order to examine the weathering effect on ^{40}Ar - ^{39}Ar ages of Antarctic meteorites, the ^{40}Ar - ^{39}Ar age patterns were compared for the outer and inner portions of two Antarctic meteorites (ALH-761, ALH-77288).

The results indicate that the oxidized outer portions show anomalously old ^{40}Ar - ^{39}Ar ages which exceed 4600 Ma in the intermediate temperature fractions of around 800-1000°C. These old ^{40}Ar - ^{39}Ar ages are accompanied by the increase of ^{36}Ar , which is regarded to be mostly of atmospheric ^{36}Ar . This might be explained by the incorporation of atmospheric Ar in hematite which was produced from goethite during neutron irradiation.

The inner relatively fresh portions show the following plateau ages: ALH-761,64, 4487 ± 50 Ma; ALH-77288,63, 4497 ± 40 Ma.

1. Introduction

Since the accidental discovery of 9 meteorites on bare ice near the Yamato Mountains, East Antarctica, by the Japanese Antarctic Research Expedition (YOSHIDA *et al.*, 1971), more than 5000 meteorites have been found by a series of meteorite search teams in Antarctica (*e.g.*, CASSIDY *et al.*, 1977; YANAI and NAGATA, 1982). They include most kinds of meteorites so far reported from the other areas and also many pieces of rare or new types of meteorites (YANAI and NAGATA, 1982). Hence, they surely add abundant treasure for meteorite research.

The meteorites were found on ice surfaces and their terrestrial ages have been estimated to be mostly of more than 10^3 years (*e.g.*, FIREMAN, 1982; FIREMAN *et al.*, 1979; HONDA, 1981; NISHIZUMI *et al.*, 1979). Hence, they are regarded to have been affected by the weathering to some extent. Such weathering effects on the chemical and mineral compositions have been reported (*e.g.*, GIBSON and KOTRA, 1982; GOODING, 1981; OLSEN *et al.*, 1978). However, such effects on radiometric ages have not yet been studied in detail. Although we try to use the most fresh portion in a meteorite specimen, it does not always guarantee that the selected portion is sufficiently fresh to get reliable radiometric ages. In the case of K-Ar systematics, such effects will be more severe compared with solid elements like Rb-Sr or Sm-Nd. So far, we have determined the radiometric ages of more than ten Antarctic meteorites by the ^{40}Ar - ^{39}Ar method (KANEOKA, 1980, 1981; KANEOKA *et al.*, 1979). The results seem to show an influence of weathering to some extent in a few cases. Hence, it is essential to examine the effect in more detail by comparing the ^{40}Ar - ^{39}Ar ages between the fresh and the weathered portions from the same material. In this context, Antarctic meteorites offer us a

unique opportunity for examining the effect of weathering, because some relatively large specimens are available for this purpose.

In the present study, two relatively large Antarctic meteorites were selected and the outer and the inner portions were used for ^{40}Ar - ^{39}Ar age determinations and their results are compared in order to examine the weathering effects on the ^{40}Ar - ^{39}Ar ages.

2. Samples

Two samples were selected for the present purpose on the basis of their relatively large sizes (original diameter, more than 10 cm), the apparently weathered surface portions with fresher inner portions and their availability.

The sample Allan Hills-761 (ALH-761) is an L6 chondrite whose schematic outline is sketched in Fig. 1. It is partly covered with fusion crusts. In the outer portions,

ALH-761 (L6)

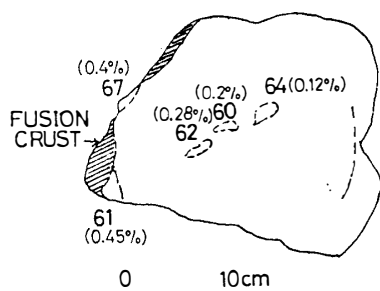


Fig. 1. The schematic sketch of the sample ALH-761(L6). The number indicates each portion. The portions 60 and 67 were used for chemical analyses (HARAMURA, personal commun., 1982). In the present study, the portions 61, 62 and 64 were used. The numerical figures in parentheses indicate $\text{H}_2\text{O}(+)$ contents for each portion.

it has rusty parts which are regarded to be secondarily formed goethite. Even in the intermediate portion, such parts are observed. This sample had been separated into two parts and each of them has been kept at the National Institute of Polar Research, Japan and at the U.S.A. side, respectively. From the cut surface, samples 61, 62 and 64 were taken away for the present purpose. The portions 60 and 67 were used for chemical analyses of major elements by HARAMURA. According to his results (HARAMURA, personal commun., 1982), no large difference is observed in the major components between 60 and 67 except for the $\text{H}_2\text{O}(+)$ content.

The other sample Allan Hills-77288 (ALH-77288) is an H6 chondrite, whose sche-

ALH-77288 (H6)

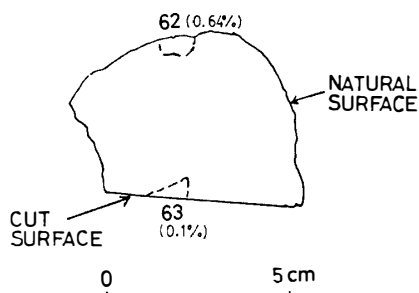


Fig. 2. The schematic sketch of the sample ALH-77288 (H6). Cut surface indicates that the other half was already detached from this block. The meanings of numerical figures are the same as in Fig. 1.

matic outline is shown in Fig. 2. This sample had also been separated into two parts to be allocated to the Japan and the U.S.A. sides, respectively. As shown in Fig. 2, the cut surface is the part which corresponds to almost the innermost part for the sample. From this sample, two portions 62 and 63 were adopted for the present purpose. As described above, the portion 63 should represent a relatively fresh part of this meteorite, whereas the portion 62 should indicate the most weathered part. This sample also has some rusty parts in the outer portions.

3. Experimental Procedures

Each sample was arranged into grains of roughly 1–5 mm in size and wrapped in aluminium foil. They were stacked together with age standards MMhb-1 (hornblende, K-Ar age: 519.5 ± 2.5 Ma) (ALEXANDER *et al.*, 1978) on both sides to be able to monitor the neutron flux gradients, remelted CaF_2 and K_2SO_4 for estimating the correction factors for Ca- and K-derived interference Ar isotopes. They were vacuum sealed in quartz vials.

Samples were irradiated in the JMTR of Tohoku University for 25 days with the total fast neutron flux of 1.1×10^{19} nvt. After the cooling for 4 months, they were degassed and Ar isotopes were analyzed on a Reynolds type mass spectrometer (60°, 15 cm) with a Farady cup. Such experimental procedures were almost the same as those reported before (KANEOKA, 1980, 1981; KANEOKA *et al.*, 1979).

Before each sample analysis, blanks were taken and applied for the correction of the data. Blank levels are $(2-4) \times 10^{-8}$ cm³ STP ^{40}Ar below 1300°C, but increase up to $(7-9) \times 10^{-8}$ cm³ STP at the highest temperature (1550°C) for 45 minutes.

The amounts of Ar were estimated on the basis of the sensitivity of the mass spectrometer which was calibrated by the amount of radiogenic ^{40}Ar in the standard sample. They include the uncertainty of about 30% based on their reproducibility. Mass discrimination among Ar isotopes ranged from 0.13% to 0.28% per atomic mass unit favoring lighter isotopes during the analyses for the present samples.

Based on the analyses of the CaF_2 and K_2SO_4 , the following correction factors were determined for Ca- and K-derived interference Ar isotopes.

$$\begin{aligned} (^{39}\text{Ar}/^{37}\text{Ar})_{\text{Ca}} &= (11.3 \pm 0.4) \times 10^{-4}, \\ (^{38}\text{Ar}/^{37}\text{Ar})_{\text{Ca}} &= (2.06 \pm 0.03) \times 10^{-3}, \\ (^{36}\text{Ar}/^{37}\text{Ar})_{\text{Ca}} &= (3.72 \pm 0.06) \times 10^{-4}, \\ (^{40}\text{Ar}/^{39}\text{Ar})_{\text{K}} &= (19.6 \pm 0.4) \times 10^{-2}, \end{aligned}$$

and

$$(^{38}\text{Ar}/^{39}\text{Ar})_{\text{K}} = (3.47 \pm 0.04) \times 10^{-2}.$$

The amounts of trapped and spallogenic components were calculated by assuming that the $^{38}\text{Ar}/^{36}\text{Ar}$ ratios for trapped and spallogenic components are 0.187 and 1.5, respectively. ^{40}Ar was corrected for trapped ($^{40}\text{Ar}/^{36}\text{Ar} = 0.5 \pm 0.5$) and spallogenic ($^{40}\text{Ar}/^{36}\text{Ar} = 0.15 \pm 0.15$) components (PODOSEK and HUNEKE, 1973). In the present study, many fractions show that the $^{38}\text{Ar}/^{36}\text{Ar}$ ratio exceeds 1.5. In such a case, excess ^{38}Ar would be attributed to the production of ^{38}Ar by a reaction $^{37}\text{Cl}(n, \gamma\beta) ^{38}\text{Ar}$ and the remainder spallogenic. However, this assumption seems to be not always guaranteed in the present case due to relatively high neutron flux on samples. Hence, no expo-

sure ages are reported in the present study.

In order to identify the state of the sample, the H₂O content was measured by using the Karl-Fisher titration method for each portion. In this case, about a few mg of the aliquots of samples were used for H₂O measurements.

4. Results

All observed Ar isotopes and calculated ⁴⁰Ar-³⁹Ar ages are tabulated in Table 1 for each phase. Furthermore, the measured H₂O content and the estimated K- and Ca-contents are summarized in Table 2 together with the summary of some characteristic ⁴⁰Ar-³⁹Ar ages for each sample.

4.1. H₂O contents

The H₂O(+) content was estimated as the difference between the measured total H₂O content and the H₂O(−) content for a sample. In Figs. 1 and 2, the H₂O(+) content is shown to demonstrate its variation at a different portion in a sample. For example, in the case of ALH-761, the outer portions show larger amounts of H₂O(+) compared with the inner portions. This trend is consistent with the apparent difference in the amount of oxidized part for the sample. This means that the oxidized part probably includes some form of hydrates. Based on microscopic observations, such phase seems to be amorphous and probably be goethite or goethite-like minerals. Even the innermost portion of the sample ALH-761, the portion 64 shows the H₂O(+) content of about 0.1%. Since the sample ALH-761 is an L6 chondrite, this amount is still too large to be accepted as completely fresh for this portion. This means that even the innermost portion might have been weathered to some extent.

For the sample ALH-77288, a similar tendency is observed. The outer portion 62 shows a larger H₂O(+) content of about 0.6% compared with that of the inner portion 63 (0.1%). Such difference probably reflects the different degree of the production of secondary minerals like goethite.

4.2. ⁴⁰Ar-³⁹Ar ages

In Fig. 3, ⁴⁰Ar-³⁹Ar diagrams are shown for different portions of the sample ALH-761. As shown in Fig. 3, all three portions show generally similar ⁴⁰Ar-³⁹Ar age patterns except for some temperature fractions around 1000°C. The innermost portion 64 shows a plateau age of 4487 ± 50 Ma for 900–1100°C fractions. These fractions represent about 46% of the total released ³⁹Ar. At higher temperatures, the apparent ⁴⁰Ar-³⁹Ar ages decrease until about 4200 Ma. This may partly reflect the recoil effect as suggested by HUNEKE and SMITH (1976) and partly because of insufficient correction for Ca-derived interference Ar isotopes or blanks. This portion shows a total ⁴⁰Ar-³⁹Ar age of 4417 Ma, which is slightly younger than the plateau age. Hence, small amount of radiogenic ⁴⁰Ar loss is suggested from this portion.

On the other hand, the outermost portion 61 shows no definite plateau age, but a rather slight increase in the apparent ages up to the 900°C fraction. In the 1000°C fraction, however, this portion shows an old ⁴⁰Ar-³⁹Ar age of 4679 ± 18 Ma. Even in the 1100 and 1200°C fractions, the portion 61 shows a slightly older ⁴⁰Ar-³⁹Ar age of

Table 1. Ar isotopes in neutron-irradiated meteorite samples from Antarctica.

ALH-761, 61 (L6) 0.8105 g, $J=0.05929\pm0.00046$

T (°C)	^{40}Ar ($\times 10^{-8}$ cm ³ STP/g)	$^{36}\text{Ar}/^{40}\text{Ar}$ ($\times 10^{-4}$)	$^{37}\text{Ar}/^{40}\text{Ar}$ ($\times 10^{-3}$)	$^{38}\text{Ar}/^{40}\text{Ar}$ ($\times 10^{-2}$)	$^{39}\text{Ar}/^{40}\text{Ar}$ ($\times 10^{-3}$)	$^{40}\text{Ar}^*/^{39}\text{Ar}^*$	Age (Ma)
600	253	0.5458 ± 0.1190	9.129 ± 0.461	7.960 ± 0.043	5.761 ± 0.191	173.6 ± 5.8	4373 ± 56
700	967	0.6470 ± 0.0340	6.968 ± 0.119	0.9960 ± 0.0077	5.796 ± 0.029	172.5 ± 0.9	4363 ± 15
800	1280	0.9001 ± 0.0285	6.342 ± 0.094	0.2395 ± 0.0031	5.656 ± 0.020	176.8 ± 0.6	4403 ± 14
900	962	0.8918 ± 0.0542	9.188 ± 0.539	0.2175 ± 0.0016	5.609 ± 0.057	178.3 ± 1.8	4417 ± 21
1000	915	5.511 ± 0.045	7.683 ± 0.160	0.2862 ± 0.0019	4.790 ± 0.036	208.8 ± 1.6	4679 ± 18
1100	571	6.366 ± 0.092	21.88 ± 0.12	1.182 ± 0.004	5.235 ± 0.057	191.0 ± 2.1	4531 ± 22
1200	102	10.97 ± 0.20	39.74 ± 0.89	2.583 ± 0.026	5.252 ± 0.181	190.4 ± 6.6	4526 ± 59
1300	114	10.61 ± 1.20	128.9 ± 0.8	6.136 ± 0.025	6.378 ± 0.031	156.8 ± 0.8	4207 ± 15
1550	324	23.07 ± 0.17	403.1 ± 4.2	10.20 ± 0.10	6.684 ± 0.057	160.6 ± 1.5	4246 ± 20
Total	5488	3.871	35.51	1.585	5.558	179.9	4431

ALH-761,62 (L6) 0.5416 g, $J=0.06098\pm0.00041$

T (°C)	^{40}Ar ($\times 10^{-8}$ cm ³ STP/g)	$^{36}\text{Ar}/^{40}\text{Ar}$ ($\times 10^{-4}$)	$^{37}\text{Ar}/^{40}\text{Ar}$ ($\times 10^{-3}$)	$^{38}\text{Ar}/^{40}\text{Ar}$ ($\times 10^{-2}$)	$^{39}\text{Ar}/^{40}\text{Ar}$ ($\times 10^{-3}$)	$^{40}\text{Ar}^*/^{39}\text{Ar}^*$	Age (Ma)
600	112	4.477 ± 0.288	15.59 ± 1.07	12.48 ± 0.03	5.914 ± 0.480	169.6 ± 13.8	4381 ± 134
700	770	0.9416 ± 0.0395	7.880 ± 0.219	1.278 ± 0.017	5.979 ± 0.111	167.5 ± 3.1	4361 ± 32
800	1064	0.7748 ± 0.0705	6.313 ± 0.402	0.3128 ± 0.0050	5.725 ± 0.070	174.9 ± 2.1	4432 ± 21
900	1592	0.7270 ± 0.0493	6.541 ± 0.236	0.3293 ± 0.0049	5.526 ± 0.048	181.2 ± 1.6	4490 ± 18
1000	1632	8.621 ± 0.069	6.051 ± 0.105	0.4629 ± 0.0154	4.295 ± 0.033	233.2 ± 1.8	4912 ± 17
1100	540	3.707 ± 0.166	19.53 ± 1.20	1.867 ± 0.017	5.481 ± 0.122	183.2 ± 4.1	4508 ± 39
1200	184	8.880 ± 0.190	65.55 ± 1.84	6.622 ± 0.016	5.563 ± 0.163	182.2 ± 5.4	4499 ± 50
1300	155	16.78 ± 0.61	247.9 ± 2.4	12.09 ± 0.15	6.712 ± 0.251	155.5 ± 6.1	4239 ± 65
1550	286	40.22 ± 0.50	500.6 ± 2.6	15.55 ± 0.12	5.338 ± 0.450	209.6 ± 24.4	4732 ± 177
Total	6335	5.533	37.78	1.987	5.322	191.3	4579

Table 1. Continued.

ALH-761,64 (L6) 0.6981 g, $J=0.06276\pm0.00037$

T (°C)	[⁴⁰ Ar] ($\times 10^{-8}$ cm ³ STP/g)	³⁶ Ar/ ⁴⁰ Ar ($\times 10^{-4}$)	³⁷ Ar/ ⁴⁰ Ar ($\times 10^{-3}$)	³⁸ Ar/ ⁴⁰ Ar ($\times 10^{-2}$)	³⁹ Ar/ ⁴⁰ Ar ($\times 10^{-3}$)	⁴⁰ Ar*/ ³⁹ Ar*	Age (Ma)
600	289	2.578	9.762	4.617	6.080	164.8	4381
		± 0.079	± 0.199	± 0.011	± 0.047	± 1.3	± 16
700	636	0.9424	6.711	0.8142	5.778	173.3	4464
		± 0.1681	± 0.550	± 0.0128	± 0.085	± 2.6	± 24
800	1405	0.6131	7.037	0.2931	5.967	167.8	4411
		± 0.0296	± 0.063	± 0.0017	± 0.022	± 0.6	± 11
900	2008	0.6300	17.32	0.3412	5.682	176.6	4495
		± 0.0321	± 0.83	± 0.0055	± 0.082	± 2.6	± 25
1000	574	0.7743	8.889	0.4389	5.764	173.8	4469
		± 0.0755	± 0.626	± 0.0011	± 0.109	± 3.3	± 33
1100	619	1.082	9.507	0.6157	5.732	174.8	4478
		± 0.079	± 0.198	± 0.0031	± 0.090	± 2.7	± 27
1200	491	2.549	22.39	1.618	6.046	166.1	4394
		± 0.050	± 0.38	± 0.020	± 0.083	± 2.3	± 25
1300	213	9.055	106.5	4.639	6.731	151.3	4241
		± 0.069	± 1.4	± 0.025	± 0.105	± 2.4	± 28
1550	421	31.08	515.5	9.312	7.367	147.4	4199
		± 0.14	± 1.2	± 0.048	± 0.144	± 3.1	± 36
Total	6656	3.125	46.97	1.391	5.947	168.5	4417

ALH-77288,62 (H6) 0.6967 g, $J=0.04791\pm0.00029$

T (°C)	[⁴⁰ Ar] ($\times 10^{-8}$ cm ³ STP/g)	³⁶ Ar/ ⁴⁰ Ar ($\times 10^{-4}$)	³⁷ Ar/ ⁴⁰ Ar ($\times 10^{-3}$)	³⁸ Ar/ ⁴⁰ Ar ($\times 10^{-2}$)	³⁹ Ar/ ⁴⁰ Ar ($\times 10^{-3}$)	⁴⁰ Ar*/ ³⁹ Ar*	Age (Ma)
600	34.7	26.48	49.74	33.38	5.107	198.0	4240
		± 0.36	± 1.34	± 0.25	± 0.198	± 7.8	± 65
700	111	4.131	158.5	4.090	4.346	240.0	4556
		± 0.138	± 3.9	± 0.040	± 0.085	± 4.9	± 35
800	1613	9.622	3.748	0.1767	2.974	336.7	5125
		± 0.110	± 0.087	± 0.0020	± 0.059	± 6.7	± 35
900	487	33.05	1.353	0.05202	(0.1046)	(9699)	(11083)
		± 0.32	± 0.052	± 0.00786	(± 0.0621)	(± 5842)	(± 1084)
1000	1018	0.5700	7.229	0.2304	4.365	229.5	4482
		± 0.0408	± 0.208	± 0.0021	± 0.113	± 6.0	± 44
1100	528	1.452	15.72	1.076	4.466	224.8	4448
		± 0.068	± 0.55	± 0.009	± 0.183	± 4.2	± 33
1200	275	2.357	31.95	1.681	4.349	231.9	4499
		± 0.150	± 0.82	± 0.005	± 0.164	± 8.8	± 65
1300	644	3.246	52.12	1.828	4.434	228.6	4476
		± 0.109	± 0.59	± 0.013	± 0.071	± 3.7	± 29
1550	1231	13.80	96.67	2.222	4.278	263.6	4555
		± 0.08	± 0.64	± 0.008	± 0.045	± 3.1	± 128
Total	5941.7	9.079	34.18	1.200	3.636	271.0	4759

Table 1. Continued.

ALH-77288,63 (H6) 0.6977 g, $J=0.04791\pm0.00029$

T (°C)	[^{40}Ar] ($\times 10^{-8}$ cm 3 STP/g)	$^{36}\text{Ar}/^{40}\text{Ar}$ ($\times 10^{-4}$)	$^{37}\text{Ar}/^{40}\text{Ar}$ ($\times 10^{-3}$)	$^{38}\text{Ar}/^{40}\text{Ar}$ ($\times 10^{-2}$)	$^{39}\text{Ar}/^{40}\text{Ar}$ ($\times 10^{-3}$)	$^{40}\text{Ar}^*/^{39}\text{Ar}^*$	Age (Ma)
600	90.6	26.70 ± 0.59	-0.0656 ± 0.1587	0.2518 ± 0.0361	1.357 ± 0.201	736.7 ± 109.1	6479 ± 260
700	204	2.202 ± 0.195	1.845 ± 0.070	0.1082 ± 0.0249	4.087 ± 0.144	244.7 ± 8.6	4588 ± 59
800	619	0.8095 ± 0.1089	5.218 ± 0.447	0.05865 ± 0.00676	4.118 ± 0.072	243.2 ± 4.3	4578 ± 31
900	666	0.5460 ± 0.0638	3.447 ± 0.430	0.04560 ± 0.00692	4.015 ± 0.101	249.3 ± 6.3	4619 ± 43
1000	1123	0.4472 ± 0.0409	4.348 ± 0.670	0.07443 ± 0.00388	4.281 ± 0.098	233.6 ± 5.3	4511 ± 39
1100	894	1.345 ± 0.052	10.70 ± 0.30	0.3425 ± 0.0110	4.321 ± 0.039	232.1 ± 2.1	4501 ± 18
1200	189	2.403 ± 0.161	21.79 ± 1.01	0.8116 ± 0.0500	4.550 ± 0.100	225.0 ± 5.1	4449 ± 39
1300	384	4.519 ± 0.105	41.39 ± 0.75	1.360 ± 0.004	4.362 ± 0.024	231.7 ± 1.3	4498 ± 14
1550	2480	9.362 ± 0.043	69.93 ± 0.45	1.771 ± 0.015	4.047 ± 0.094	252.0 ± 6.0	4637 ± 41
Total	6649.6	4.773	32.13	0.8376	4.167	271.9	4764

- 1) All tabulated data have been corrected for the blanks and radioactive decay to ^{37}Ar between irradiation and analysis, but do not include other corrections.
- 2) $^{40}\text{Ar}^*/^{39}\text{Ar}^*$ indicates a ratio of the radiogenic ^{40}Ar from the decay of ^{40}K ($=^{40}\text{Ar}^*$) to the K-derived ^{39}Ar by a reaction of ^{39}K (n, p) ^{39}Ar ($=^{39}\text{Ar}^*$).
- 3) The uncertainty represents one standard deviation.

Table 2. Summary of ^{40}Ar - ^{39}Ar ages of Antarctic meteorites.

Sample	[K]* (%)	[Ca]* (%)	H_2O (+)** (%)	H_2O (-) (%)	Total	^{40}Ar - ^{39}Ar age (Ma)***			Plateau range
						Min	Max	Plateau	
ALH-761 (L6)									
61	0.073	0.89	0.45	0.29	4431	4207 ± 15	4679 ± 18	—	—
62	0.081	1.1	0.28	0.43	4579	4239 ± 65	4912 ± 17	—	—
64	0.095	1.4	0.12	0.58	4417	4199 ± 36	4495 ± 25	4487 ± 50	900-1100°C (46.2% of released ^{39}Ar)
ALH-77288									
62 (H6)	0.052	0.93	0.64	0.48	4759	4240 ± 65	11083 ± 1084	4466 ± 50	1000-1300°C (49.4% of released ^{39}Ar)
63	0.067	0.98	(0.1)	(1.5)	4764	4449 ± 39	6479 ± 260	4497 ± 40	1000-1300°C (41.6% of released ^{39}Ar)

* K- and Ca-contents were estimated based on the total amounts of ^{39}Ar and ^{37}Ar of samples by comparing those of the standard sample MMhb-1. About 30% uncertainty is included in each value.

** H_2O (+) contents were calculated by measuring total H_2O and H_2O (-) contents based on Karl-Fisher titration method (TIBA, personal commun., 1983).

*** ^{40}Ar - ^{39}Ar age was calculated by using following constants for ^{40}K (STEIGER and JÄGER, 1977).
 $\lambda_e=0.581\times 10^{-10}\text{ yr}^{-1}$, $\lambda_\beta=4.962\times 10^{-10}\text{ yr}^{-1}$, $^{40}\text{K}/\text{K}=1.167\times 10^{-4}$.
 Uncertainties in the ages correspond to 1σ .

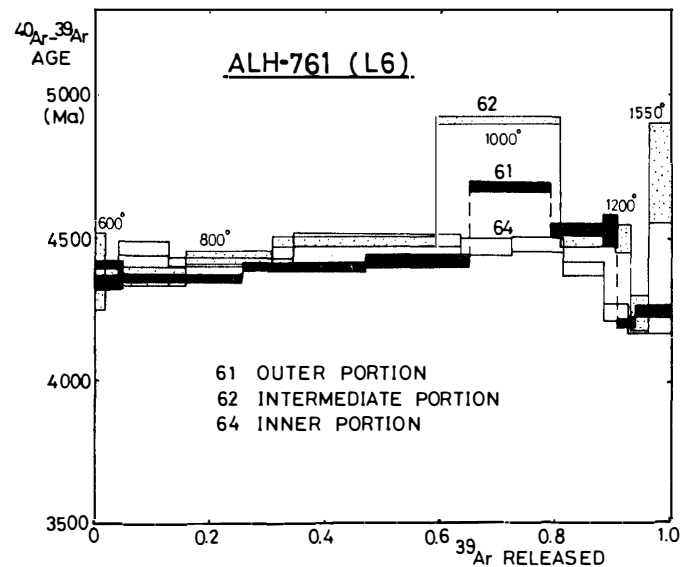


Fig. 3. The ^{40}Ar - ^{39}Ar age diagrams for the sample ALH-761. The uncertainties in the ^{40}Ar - ^{39}Ar ages represent 1σ . Note the anomalously old ^{40}Ar - ^{39}Ar ages in the 1000°C fractions for the portions 62 and 61.

about 4530 Ma compared with the plateau age of the portion 64. In the 1300 and 1550°C fractions, the apparent ^{40}Ar - ^{39}Ar ages decrease suddenly down to about 4200 Ma. The apparent decrease in ^{40}Ar - ^{39}Ar ages at higher temperatures would probably be attributed to the same reason as for the portion 64. However, the apparently old ^{40}Ar - ^{39}Ar age which exceeds 4600 Ma requires some explanation.

The intermediate portion 62 also shows an anomalously old ^{40}Ar - ^{39}Ar age in the 1000°C fraction. In this case, the apparent ^{40}Ar - ^{39}Ar age becomes up to 4900 Ma. In the 1300°C fraction, this portion also shows a young ^{40}Ar - ^{39}Ar age of about 4240 Ma. In the 1550°C fraction, the ^{40}Ar - ^{39}Ar age increases to 4732 Ma. However, the analytical uncertainty in the age is relatively large for this fraction (177 Ma as 1σ). Hence, we cannot regard this apparently old ^{40}Ar - ^{39}Ar age as a real one. Probably, we can attribute the apparent variation in the observed ages at higher temperatures to the same reason as for the other two portions. However, the apparently old ^{40}Ar - ^{39}Ar ages seen at the same intermediate temperature around 1000°C as the portion 61 require some other explanation. The portions 61 and 62 include oxidized parts and contain larger amounts of $\text{H}_2\text{O}(+)$, which suggests that these portions might have been affected by weathering to some extent. The relatively fresh part 64 shows a plateau age without showing any such old ^{40}Ar - ^{39}Ar age even in the 1000°C fraction. Hence, the apparently old ^{40}Ar - ^{39}Ar ages for the fractions around 1000°C of the outermost and the intermediate portions 61 and 62 seem to be related to some secondary effects caused by the weathering of the specimen. This point will be discussed later.

In Fig. 4, the ^{40}Ar - ^{39}Ar age diagrams for the sample ALH-77288 are shown. The inner portion 63 shows a slightly older ^{40}Ar - ^{39}Ar age at lower temperatures, but indicates a plateau age of 4497 ± 40 Ma for 1000–1300°C, which covers about 42% of the released total ^{39}Ar . At the highest temperature, it shows an old ^{40}Ar - ^{39}Ar age of 4637 ± 41

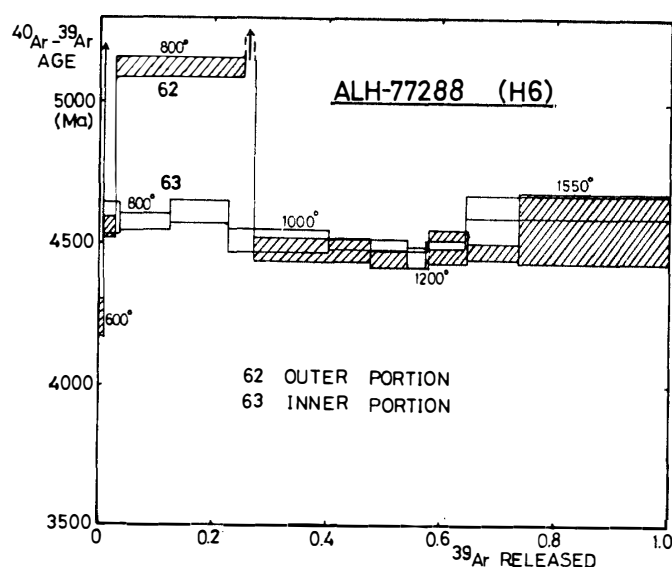


Fig. 4. The ^{40}Ar - ^{39}Ar age diagrams for the sample ALH-77288. Note the anomalously old ^{40}Ar - ^{39}Ar ages in the 800 and 900°C fractions for the portion 62. For the portion 63, these temperature fractions also show slightly older ^{40}Ar - ^{39}Ar ages than the higher temperatures. The apparently old ^{40}Ar - ^{39}Ar ages in the highest temperature fractions for both portions 62 and 63 include relatively large uncertainties of Ca-derived interference Ar isotopes together with blank corrections. Hence, these cases are not discussed in detail in the text.

Ma, which seems too old to be accepted as a meaningful age. Since the highest temperature fraction is most easily affected by the experimental uncertainties caused by the corrections for Ca-derived interference Ar isotopes and blanks, we cannot take the face value for this fraction seriously, unless it shows a moderate value. For this sample, the lowest temperature fraction shows a very old ^{40}Ar - ^{39}Ar age of 6479 ± 260 Ma, which probably reflects an atmospheric contamination.

On the other hand, the sample ALH-77288,62 indicates an anomalously old ^{40}Ar - ^{39}Ar age of more than 11000 Ma in the 900°C fraction. Even in the 800°C fraction, the apparent ^{40}Ar - ^{39}Ar age corresponds to 5125 ± 35 Ma. These old ages cannot be regarded to have any chronological significance, because they appear only in the limited portion of a sample, where some weathering effects seem to have worked. For this sample, an apparent plateau age of 4466 ± 50 Ma is obtained for 1000–1300°C, which corresponds to about 49% of the total released ^{39}Ar and agrees with that of the portion 63 within their analytical uncertainties.

As shown above for both samples ALH-761 and ALH-77288, the anomalously old ^{40}Ar - ^{39}Ar ages which exceed 4600 Ma are observed only in such portions that seem to have been affected by weathering to some extent. No such old ^{40}Ar - ^{39}Ar ages have been observed in relatively fresh portions except for the lowest temperature fraction for the sample ALH-77288,63. Hence, it is reasonable to assume that such apparently too old ^{40}Ar - ^{39}Ar ages should reflect some state of samples resulting from weathering of the samples. Terrestrial atmospheric contamination is the most likely effect to

explain such old ^{40}Ar - ^{39}Ar ages and this point shall be discussed in more detail later.

4.3. Release patterns of Ar isotopes

As shown in Figs. 3 and 4, anomalously old ^{40}Ar - ^{39}Ar ages are observed for some

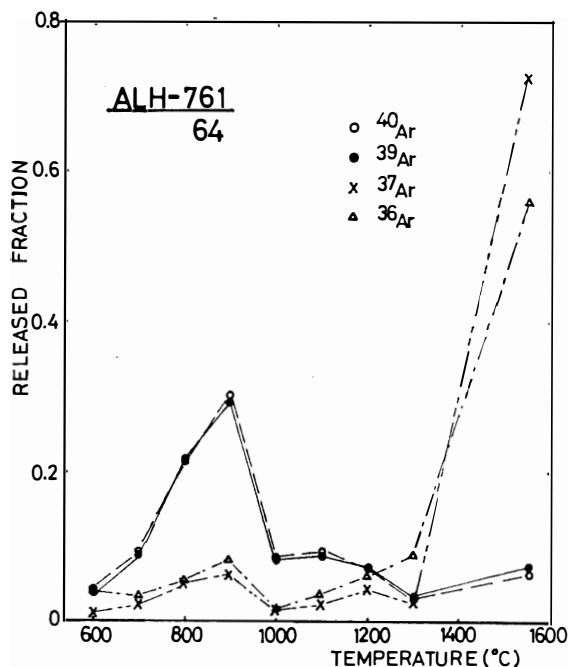


Fig. 5a. The release patterns of Ar for the sample ALH-761, 64. Note the good correlation between ^{40}Ar and ^{39}Ar .

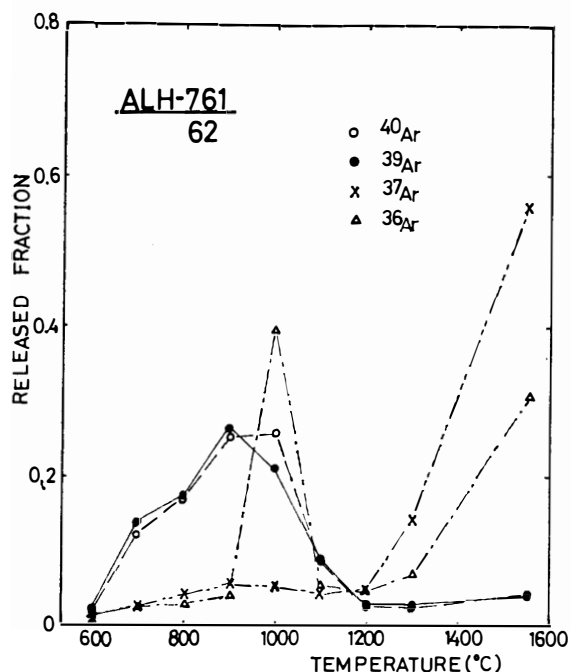


Fig. 5b. The release patterns of Ar for the sample ALH-761,62. Note the anomalously large increase of ^{36}Ar at 1000°C with a slight deviation of ^{40}Ar from ^{39}Ar release pattern at the same temperature.

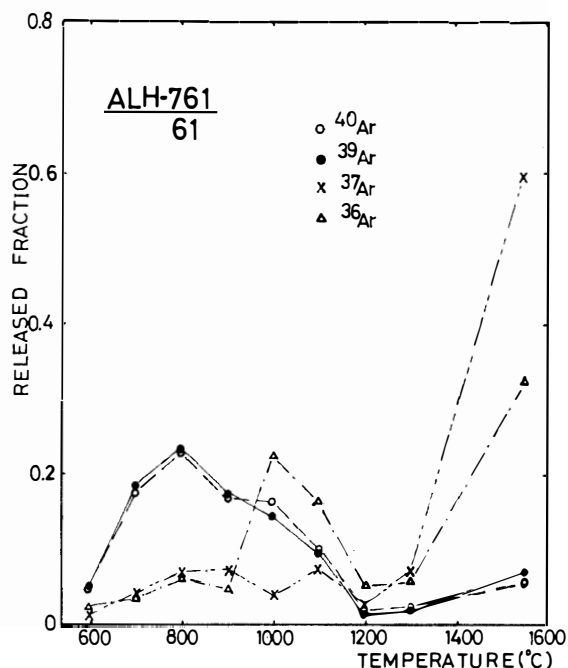


Fig. 5c. The release patterns of Ar for the sample ALH-761, 61. At 1000°C and 1100°C , a large increase of ^{36}Ar is observed, which is correlated with the increase of apparent ^{40}Ar - ^{39}Ar ages in Fig. 3.

portions which seem to have been affected by weathering. In this context, it is interesting to compare the release patterns of Ar isotopes for portions which include both the weathered and relatively fresh ones.

In Fig. 5a, the release patterns of Ar isotopes for ALH-761,64 are shown. ^{40}Ar and ^{39}Ar show almost similar release patterns with the largest release at 900°C. On the other hand, large fractions of more than 50% of Ar were degassed at the highest temperature (1550°C) for both ^{37}Ar and ^{38}Ar . Since ^{37}Ar is a Ca-derived component, this indicates that ^{36}Ar would also be trapped in a phase in which most Ca is included. Although slight increase is observed at 900°C in the released fraction for both ^{37}Ar and ^{36}Ar , those fractions do not exceed 10% for both Ar isotopes.

In contrast with the sample ALH-761,64 the portion 62 shows a completely different release pattern of ^{36}Ar . As shown in Fig. 5b, the released fraction of ^{36}Ar is anomalously high at 1000°C, where the apparent old ^{40}Ar - ^{39}Ar age is observed in Fig. 3 for this portion. About 40% of ^{36}Ar is degassed at 900°C, whereas other Ar isotopes generally show similar release patterns to the portion 64. The released fraction of ^{40}Ar is slightly different from that of ^{39}Ar at 900°C.

For the sample ALH-761,61, the obtained release patterns of Ar are similar to those of the portion 62 (Fig. 5c). In this case, ^{36}Ar of more than 15% is degassed at 900 and 1000°C at which temperatures old ^{40}Ar - ^{39}Ar ages are observed for this portion in Fig. 3. The release patterns of ^{40}Ar and ^{39}Ar are almost similar to each other. ^{37}Ar shows almost the same release pattern to those for the portions 64 and 62.

These results on the release patterns of Ar isotopes imply that anomalously old ^{40}Ar - ^{39}Ar ages observed at around 1000°C for the samples ALH-761,62 and 61 are correlated with the large increase of the ^{36}Ar degassing at the same temperature. Since the relatively fresh innermost portion 64 shows no such trend, the apparent old ^{40}Ar - ^{39}Ar age and the increase of the ^{36}Ar seem to be related to some weathering effect like the addition of atmospheric components. However, such components are generally expected to be degassed at lower temperatures. Hence, the problem remains why such components are degassed at intermediate temperatures around 1000°C for the samples ALH-761,62 and 61.

In the case of the sample ALH-77288, a similar phenomenon is observed. In Fig. 6a, the release patterns of Ar isotopes for the inner portion 63 are shown. The release patterns of ^{40}Ar are correlated well with those of ^{39}Ar . Large amounts of ^{37}Ar and ^{36}Ar of more than 70% of the total amounts are degassed at the highest temperature. At the lowest temperature, ^{36}Ar is degassed about 10%. Such an increase in the ^{36}Ar degassing seems to reflect an apparently old ^{40}Ar - ^{36}Ar age in the 600°C fraction for this sample (Table 1). Except for the 600°C fraction, the release patterns of ^{37}Ar and ^{36}Ar are correlated well with each other.

Compared with the inner portion 63, the outer portion 62 shows more complicated release patterns. Although two peaks are observed for both ^{40}Ar and ^{39}Ar in the released patterns at 800 and 1000°C, their release patterns generally show almost the same variations in Fig. 6b. The release pattern of ^{37}Ar is also similar to that of the other portion 63. However, the released fractions of ^{36}Ar increase up to about 30% at 800 and 900°C. Anomalously old ^{40}Ar - ^{39}Ar ages are also observed in these temperature fractions. Hence, anomalously old ^{40}Ar - ^{39}Ar ages again are correlated with the large

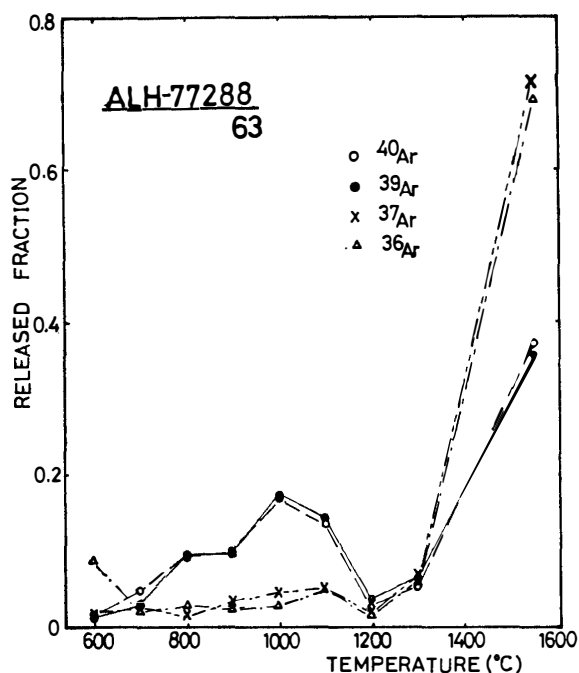


Fig. 6a. The release patterns of Ar for the sample ALH-77288, 63. For this sample, a slight increase in the ^{36}Ar degassing is observed at 600°C , which is corrected in the observed old ^{40}Ar - ^{39}Ar age at the same temperature.

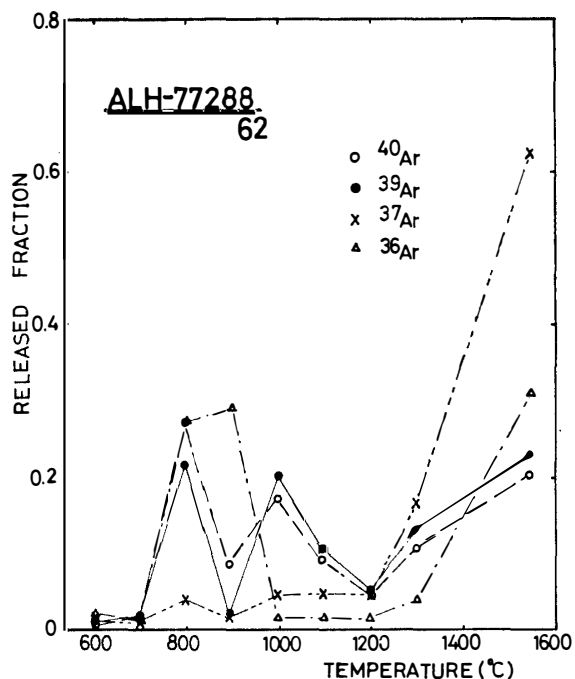


Fig. 6b. The release patterns of Ar for the sample ALH-77288, 62. At 800°C and 900°C , a large increase in the ^{36}Ar degassing is observed, which is correlated with the anomalously old ^{40}Ar - ^{39}Ar ages observed at the same temperatures.

fraction of ^{36}Ar in the intermediate temperature fractions. Since such a phenomenon is observed only for the outer portion 62 of the sample ALH-77288, it is conjectured to be related to the weathering effect like the addition of the atmospheric Ar for this portion. This is the same tendency as the sample ALH-761. Then, it is necessary to explain why such an effect due to the atmospheric contamination is observed at the intermediate temperatures instead of at the lower temperatures. This point shall be discussed later.

4.4. K and Ca concentrations

The K- and Ca-contents for each portion of the two samples were estimated based on the comparison of the total amounts of K-derived ^{39}Ar and Ca-derived ^{37}Ar of a specimen with those of the standard sample MMhb-1.

The following relationship is observed for the present samples:

$$\text{K/Ca} = (0.53 \pm 0.02) {}^{39}\text{Ar}^* / {}^{37}\text{Ar}.$$

This is almost the same value as reported before (KANEOKA, 1980, 1981; KANEOKA *et al.*, 1979).

In Table 2, the estimated K- and Ca-contents are summarized together with ^{40}Ar - ^{39}Ar ages. Apparently, both K- and Ca-contents seem to decrease from the inner portion to the outer portion systematically. One may argue that this reflects some weath-

ering effects on the chemical compositions. Since these values include the analytical uncertainty of about 30%, however, it is difficult to attribute any significance in the apparent differences in the observed data.

5. Discussion

As shown in the previous section, the present samples indicate plateau ages for the relatively fresh inner portions at higher temperatures. However, the apparently oxidized outer portions show anomalously old ^{40}Ar - ^{39}Ar ages in the intermediate fractions around 800–1000°C. Furthermore, they are accompanied by the increase in the released fraction of ^{36}Ar . When such an increase in the apparent ^{40}Ar - ^{39}Ar age is observed to be accompanied by that of ^{36}Ar in the lower temperature fraction, it is common to attribute the effect to the terrestrial atmospheric contamination on the sample. For example, the old ^{40}Ar - ^{39}Ar age in the 600°C fraction of the sample ALH-77288,63 can be explained by this mechanism. Such components are regarded to be retained in a phase which was formed secondarily and to be adsorbed on the surface, but cannot be desorbed during the preheating of a sample.

In the present case, however, the old ^{40}Ar - ^{39}Ar ages which exceed 4600 Ma occur in the intermediate temperature fractions mostly. For the sample ALH-761,62, the 1000°C fraction shows an old ^{40}Ar - ^{39}Ar age of 4912 ± 17 Ma together with the abrupt increase of ^{36}Ar as shown in Fig. 5b. If we correct for the amount of ^{40}Ar by assuming that all the observed ^{36}Ar represents the atmospheric Ar, the apparent ^{40}Ar - ^{39}Ar age decreases down to 4421 Ma. Since 900 and 1100°C fractions show the ^{40}Ar - ^{39}Ar ages of 4490–4500 Ma, the corrected age for the 1000°C fraction is slightly too low, but is a reasonable value if we take into account the existence of some amount of trapped and/or cosmogenic components in this fraction. Similarly, the absurdly old ^{40}Ar - ^{39}Ar age of 11083 Ma can be decreased down to 4462 Ma for the 900°C fraction of the sample ALH-77288,62 by correcting for the amount of ^{40}Ar based on the same assumption as described above. In the same manner, all very old ^{40}Ar - ^{39}Ar ages of more than 4600 Ma are decreased down to ages with the order of 4200–4500 Ma after applying the terrestrial atmospheric air correction based on the same assumption stated above. Hence, those old ^{40}Ar - ^{39}Ar ages probably attributed to the incorporation of the terrestrial atmospheric Ar and to the calculation of ages by neglecting this effect.

Then, the problem is raised why such atmospheric components are observed in the intermediate temperatures around 800–1000°C for the present samples. Although these temperatures are slightly different between the samples ALH-761 and ALH-77288, they would probably reflect their different physical and chemical properties. If such atmospheric contamination occurred due to the adsorption of the terrestrial atmosphere on the surface of the sample or the formation of some secondary minerals, it is generally considered to be degassed at lower temperatures. Hence, to explain the present phenomenon, some phases which are more retentive for atmospheric Ar than the normal secondary minerals are required.

Related to this problem, it is noteworthy that goethite is reported to change into hematite under some conditions. TAYLOR and BURTON (1976) examined the stability of $\text{FeO} \cdot \text{OH}$ phases including goethite, which are considered to be the secondary prod-

ucts in both meteorites and lunar rocks. According to their experiments, goethite has been found to change into hematite after 125 days at 135°C and after 19 days at 165°C. Although they report only two examples concerning this reaction, it will be possible to apply for the present samples. Samples were irradiated by neutron in the JMTR for 25 days with the maximum temperature of about 300°C. Although we do not know the exact averaged temperature in the reactor, it is expected to exceed 200°C judging from the reported maximum temperature. Hence, it is quite likely that goethite has changed into hematite during neutron irradiation as is expected from the condition for the reaction (Fig. 7). Since goethite has a chemical form of $\text{FeO} \cdot \text{OH}$, it is expected

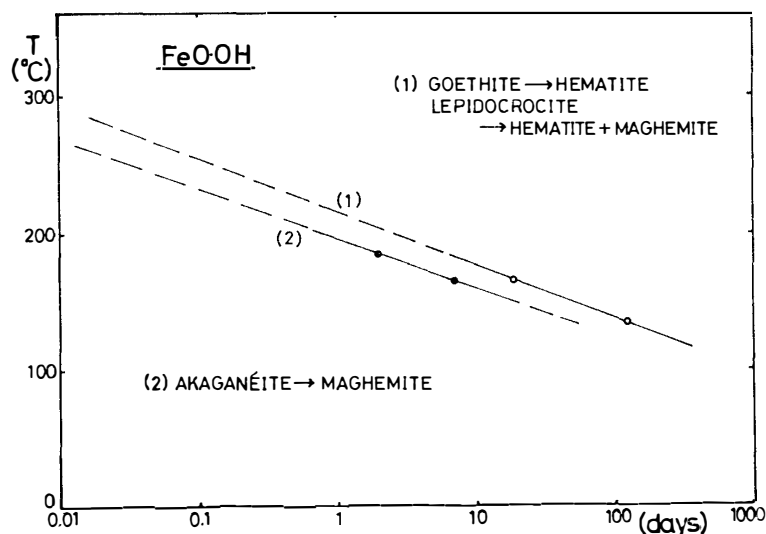


Fig. 7. The relationship between the temperature and the time for each reaction. Each line indicates that at least in the field above the line, each reaction is expected to proceed (after the data by TAYLOR and BURTON, 1976).

to contain a relatively large amount of atmospheric Ar in it and adsorb some amount on the surface due to the hydration of metal iron phase. Such atmospheric Ar would be once desorbed during the change into hematite. However, the present samples were sealed in quartz vials in vacuum, and the desorbed atmospheric Ar was kept in the quartz vials. Since hematite was formed under such a condition, it would include some amounts of atmospheric Ar during its formation. Furthermore, hematite is much more stable for temperature than goethite. Hence, the atmospheric Ar trapped in hematite will be degassed at much higher temperature compared with that of goethite. Thus, relatively high degassing temperatures of around 800–1000°C for atmospheric Ar in the present samples might be explained if we assume the process described above. Such situation is schematically shown in Fig. 8. Since we could not repeat the experiments under the same condition due to the limited availability of JMTR and the prohibition of handling the irradiated materials in the open-air to examine the structure by using X-ray analyses, the present process remains as a possibility.

These inferences suggest that such an anomalously old ^{40}Ar - ^{39}Ar age is not always limited to Antarctic meteorites but might be found in meteorites which were exposed

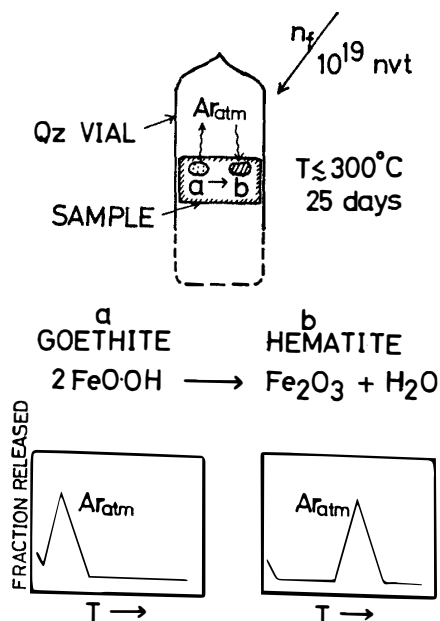


Fig. 8. Schematic diagram to show a process which might have occurred during neutron irradiation for the present samples. The lower part indicates schematic figures to show a change in the released pattern of atmospheric Ar.

on the terrestrial surface for some time during which goethite or some secondary phases are formed in it. Hence, we should be very careful in interpreting the result of ^{40}Ar - ^{39}Ar ages for such a meteorite. As shown in Fig. 8, if goethite has already changed into hematite after neutron irradiation, preheating of a meteorite sample before Ar analyses does not change the present situation. If the transformation of goethite into hematite is undertaken in vacuum at an appropriate preheating temperature before neutron irradiation, such an effect may be reduced, but we have no guarantee for the complete retention of radiogenic ^{40}Ar in that case.

Acknowledgments

I appreciate the kindness of Prof. T. NAGATA and Dr. K. YANAI of the National Institute of Polar Research in providing me the samples used in this study. Dr. YANAI offered me a special effort to prepare suitable portions of each meteorite for the present purpose. I also thank Dr. T. TIBA of the National Science Museum, who made it possible to analyze H_2O contents of the present samples by the Karl-Fisher titration method. I am grateful to Mr. H. HARAMURA of Geological Institute, University of Tokyo, who informed me of his unpublished results on chemical analyses.

This study is financially supported in part by the Ministry of Education, Science and Culture under the contract No. 00539014.

References

- ALEXANDER, E. C., Jr., MICKELSON, G. M. and LANPHERE, M. A. (1978): MMhb-1; A new ^{40}Ar - ^{39}Ar dating standard. U.S. Geol. Surv. Open-File Rep., 78-701, 6-9.
- CASSIDY, W. A., OLSEN, E. and YANAI, K. (1977): Antarctica; A deep freeze storehouse for meteorites. *Science*, **198**, 727-731.
- FIREMAN, E. L. (1982): Carbon-14 ages of Antarctic meteorites. *Meteoritics*, **17**, 212-213.
- FIREMAN, E. L., RANCITELLI, L. A. and KIRSTEN, T. (1979): Terrestrial ages of four Allan Hills meteorites; Consequences for Antarctic ice. *Science*, **203**, 453-455.

- GIBSON, E. K., Jr. and KOTRA, R. K. (1982): Organic chemistry, carbon and sulfur abundances of Antarctic meteorites; Implications for post-fall history. *Meteoritics*, **17**, 220–221.
- GOODING, J. L. (1981): Mineralogical aspects of terrestrial weathering effects in chondrites from Allan Hills, Antarctica. *Proc. Lunar Planet. Sci. Conf.* 12B, 1105–1122.
- HONDA, M. (1981): Terrestrial history of Antarctic meteorites recorded in the cosmogenic nuclides. *Geochem. J.*, **15**, 163–181.
- HUNEKE, J. C. and SMITH, S. P. (1976): The realities of recoil; ^{39}Ar recoil out of small grains and anomalous age patterns in ^{39}Ar - ^{40}Ar dating. *Proc. Lunar Sci. Conf.* 7th, 1987–2008.
- KANEOKA, I. (1980): ^{40}Ar - ^{39}Ar ages of L and LL chondrites from Allan Hills, Antarctica: ALHA-77015, 77241 and 77304. *Mem. Natl Inst. Polar Res., Spec. Issue*, **17**, 177–188.
- KANEOKA, I. (1981): ^{40}Ar - ^{39}Ar ages of Antarctic meteorites: Y-74191, Y-75258, Y-7308, Y-74450 and ALH-765. *Mem. Natl Inst. Polar Res., Spec. Issue*, **20**, 250–263.
- KANEOKA, I., OZIMA, M. and YANAGISAWA, M. (1979): ^{40}Ar - ^{39}Ar studies of four Yamato-74 meteorites. *Mem. Natl Inst. Polar Res., Spec. Issue*, **12**, 186–206.
- NISHIIZUMI, K., ARNOLD, J. R., ELMORE, D., FERRARO, R. D., GOVE, H. E., FINKEL, R. C., BEUKENS, R. P., CHANG, K. H. and KILIUS, L. R. (1979): Measurement of ^{36}Cl in Antarctic meteorites and Antarctic ice using a Van de Graaff accelerator. *Earth Planet. Sci. Lett.*, **45**, 285–292.
- OLSEN, E. J., NOONAN, A., FREDRIKSSON, K., JAROSEWICH, E. and MORELAND, G. (1978): Eleven new meteorites from Antarctica, 1976–1977. *Meteoritics*, **13**, 209–225.
- PODOSEK, F. A. and HUNEKE, J. C. (1973): Argon 40–argon 39 chronology of four calcium-rich achondrites. *Geochim. Cosmochim. Acta*, **37**, 667–684.
- STEIGER, R. H. and JÄGER, E. (1977): Subcommittee on geochronology; Convention on the use of decay constants in geo- and cosmochronology. *Earth Planet. Sci. Lett.*, **36**, 359–362.
- TAYLOR, L. A. and BURTON, J. C. (1976): Experiments on the stability of FeOOH on the surface of the moon. *Meteoritics*, **11**, 225–230.
- YANAI, K. and NAGATA, T. (1982): Collections and curation of Yamato meteorites. *Meteoritics*, **17**, 300–301.
- YOSHIDA, M., ANDO, H., OMOTO, K., NARUSE, R. and AGETA, Y. (1971): Discovery of meteorites near Yamato Mountains, East Antarctica. *Nankyoku Shiryô (Antarct. Rec.)*, **39**, 62–65.

(Received May 10, 1983; Revised manuscript received August 2, 1983)